Research article

Epigallocatechin 3-gallate inhibits the plasma membrane Ca^{2+}-ATPase: effects on calcium homeostasis

Débora E. Rinaldi [1], Mallku Q. Ontiveros [1], Nicolas A. Saffioti, Maximiliano A. Vigil, Irene C. Mangialavori, Rolando C. Rossi, Juan P. Rossi, María V. Espelt [**], Mariela S. Ferreira-Gomes [*]

IQUIFIB – Instituto de Química y Fisicoquímica Biológicas, Facultad de Farmacia y Bioquímica, Universidad de Buenos Aires, CONICET, Junín 956, 1113 Buenos Aires, Argentina

ABSTRACT

Flavonoids are natural compounds responsible for the health benefits of green tea. Some of the flavonoids present in green tea are catechins, among which are: epigallocatechin, epicatechin-3-gallate, epicatechin, catechin and epigallocatechin-3-gallate (EGCG). The latter was found to induce apoptosis, reduce reactive oxygen species, in some conditions though in others it acts as an oxidizing agent, induce cell cycle arrest, and inhibit carcinogenesis. EGCG also was found to be involved in calcium (Ca^{2+}) homeostasis in excitable and in non-excitable cells. In this study, we investigate the effect of catechins on plasma membrane Ca^{2+}-ATPase (PMCA), which is one of the main mechanisms that extrude Ca^{2+} out of the cell. Our studies comprised experiments on the isolated PMCA and on cells overexpressing the pump. Among catechins that inhibited PMCA activity, the most potent inhibitor was EGCG. EGCG inhibited PMCA activity in a reversible way favoring E1P conformation. EGCG inhibition also occurred in the presence of calmodulin, the main pump activator. Finally, the effect of EGCG on PMCA activity was studied in human embryonic kidney cells (HEK293T) that transiently overexpress hPMCA4. Results show that EGCG inhibited PMCA activity in HEK293T cells, suggesting that the effects observed on isolated PMCA occur in living cells.

1. Introduction

Flavonoids are natural compounds that belong to some plant secondary metabolites. Flavonoids have polyphenolic structures that are found in vegetables, some beverages and fruits [1]. Green tea is a flavonoid-containing beverage that has been lately receiving most attention as a health-beneficial agent. Particularly, green tea has been shown to have health benefits such as antiarthritic and anti-inflammatory effects as well as being involved in the prevention of cardiovascular diseases and cancer, among others [2, 3, 4]. Some bioactive constituents of green tea responsible for those effects are a subgroup of flavonoids called catechins, namely: epigallocatechin, epicatechin-3-gallate, epicatechin, catechin and epigallocatechin-3-gallate (EGCG) [5, 6, 7].

EGCG is the main polyphenol of green tea and it is thought to be responsible for its biological effects [5]. Many authors have shown that EGCG induces apoptosis and it has been published that in some conditions it reduces reactive oxygen species, whereas in others, it acts as an oxidizing agent [8]. Additionally, it induces cell cycle arrest, inhibits carcinogenesis [7, 9, 10], and stimulates viability and cell proliferation [11, 12]. Evidence has shown EGCG involvement in changes in calcium (Ca^{2+}) homeostasis in excitable and non-excitable cells, which could be associated to its effect on Ca^{2+} transport systems. In hippocampal cultured neurons, incubation with EGCG induced an increase in intracellular Ca^{2+} through the release from intracellular stores [13]. On the other hand, in non-excitable human astrocytoma U87 cells, EGCG increased intracellular Ca^{2+} by influx of extracellular Ca^{2+} and release from intracellular stores [14]. Furthermore, in prostate cancer cells EGCG induced an intracellular Ca^{2+} increase by a multi-step mechanism [15]. The molecular mechanisms, that involve the effects of EGCG on Ca^{2+} homeostasis, are still unclear.
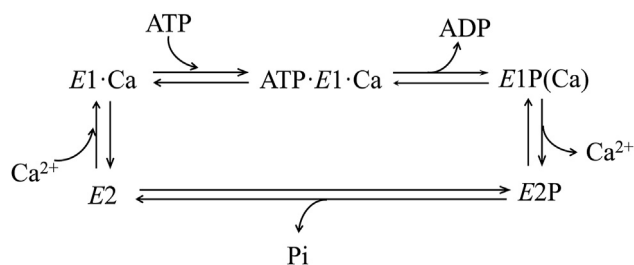

Figure 1. Simplified kinetic model of the PMCA obtained from Ontiveros et al. [17].

Ca²⁺ signaling modulates many cellular processes in most cell types. Intracellular Ca^{2+} levels are in the range of hundreds of nM in resting conditions whereas in the extracellular space its concentration is in the mM range. Although Ca^{2+} concentration inside the cell is very low, some intracellular organelles have Ca^{2+} concentrations that are close to those in the extracellular milieu, such as mitochondria or the endoplasmic reticulum (ER), the latter known as the Ca^{2+} store in the cell [16].

Excessive increases in intracellular Ca^{2+} may induce irreversible changes in cells leading them to death. To avoid those changes, cells have active mechanisms at the cell plasma membrane and at the ER membrane that maintain cytoplasmic Ca^{2+} concentrations at low levels. At the cell membrane, cells have plasma membrane Ca^{2+}-ATPase (PMCA) and the Na^+/Ca^{2+} exchanger, whereas at the ER membrane cells have the sarcoendoplasmic reticulum Ca^{2+}-ATPase (SERCA). PMCA and SERCA are P-type Ca^{2+}-ATPases that extrude Ca^{2+} out of the cytoplasm by consuming ATP. Once the ER is depleted of Ca^{2+}, store activated Ca^{2+} channels (SOCs) allow Ca^{2+} to enter the cytoplasm and Ca^{2+} pumps are activated [17].

PMCA helps to maintain intracellular Ca^{2+} at very low levels by extruding Ca^{2+} from the cytoplasm to the extracellular space. There are four PMCA isoforms encoded in different genes. Among PMCA isoforms, hPMCA4 (human isoform 4) is tightly regulated. This isoform is the most abundant in red blood cells and is ubiquitously distributed across tissues [18, 19]. PMCA contains 10 membrane-spanning segments with the N- and C-termini on the cytosolic side. In the C-terminal tail, PMCA contains an auto-inhibitory domain and a calmodulin-binding domain. Calmodulin, the main regulator of PMCA [19], binds to the corresponding C-terminal domain of the pump, modifying its activation/inactivation state.

PMCA exists in two conformational states that can be phosphorylated: $E1$ and $E2$ (Figure 1). $E1$ is phosphorylated by ATP and has high affinity for Ca^{2+}, whereas $E2$ is phosphorylated by Pi and has low affinity for Ca^{2+} [20].

Several reports have revealed that flavonoids can inhibit P- type ATPases. EGCG inhibits Na^+/K^+-ATPase by reducing the transition rate from the phosphorylated intermediate $E1P$ to $E2P$ [21]. Additionally, EGCG inhibits SERCA but has a preferential interaction with the $E2$ conformation modifying the enzyme conformation at the catalytic site [22]. Recently, we showed for the first time that some flavonoids, such as quercetin and gossypin, inhibit hPMCA4 [17]; however, the effects of catechins such as EGCG on PMCA are still unclear.
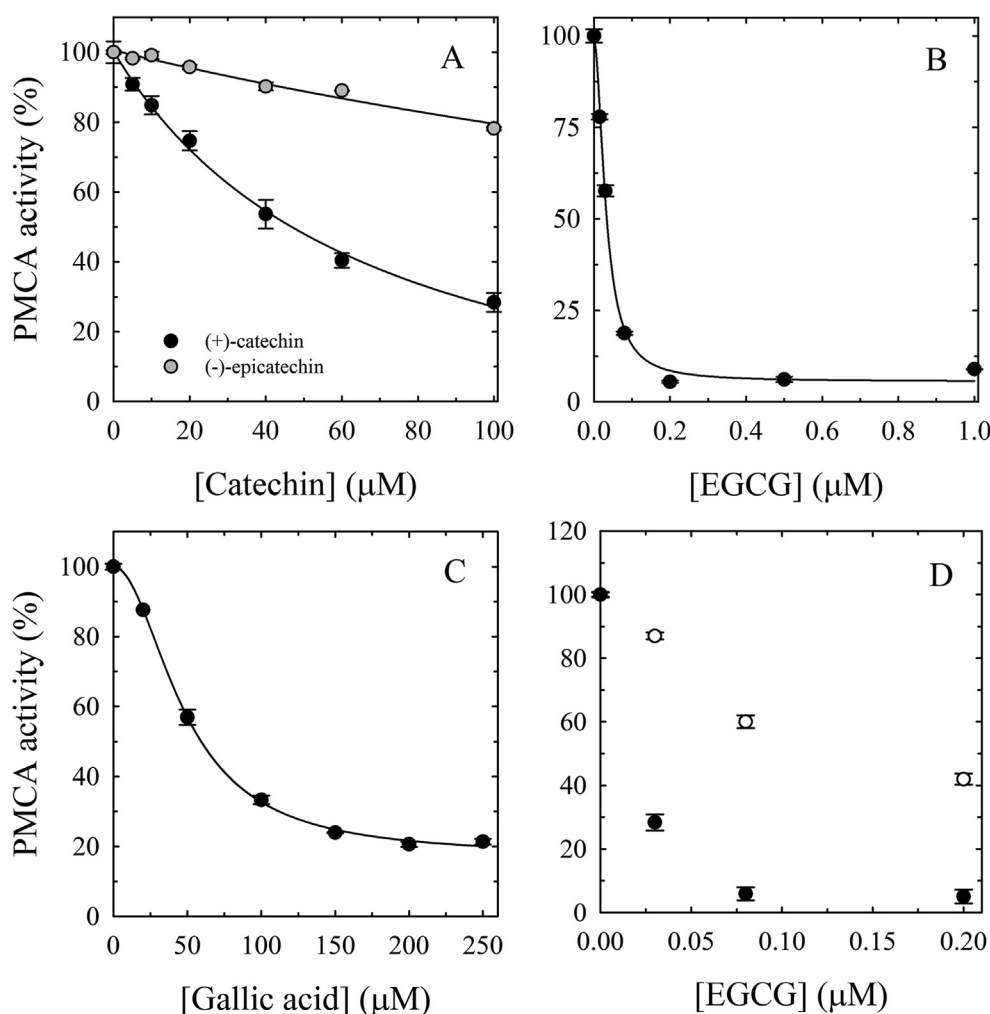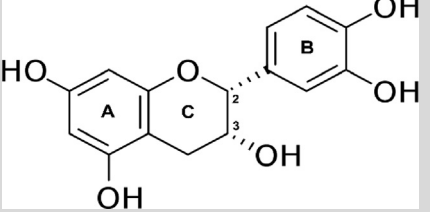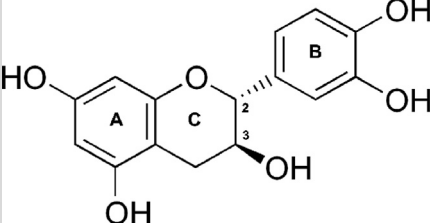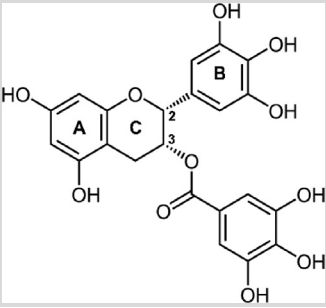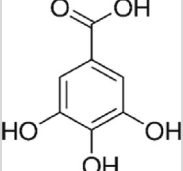

Figure 2. A-B. *Effect of catechins on PMCA activity.* PMCA activity was measured in the presence of increasing concentrations of catechins: (-)-epicatechin and (+)-catechin (A) or EGCG (B). The continuous lines in panel A represent rectangular hyperbolas (Eq. 2). The continuous line in panel B represents a Hill equation (Eq. 3). Data in A are representative of three independent experiments. Data in B are expressed as the mean ± S.E. (n = 3). C. *Effect of gallic acid on PMCA activity.* PMCA activity was measured in the presence of increasing concentrations of gallic acid. Data are representative of two independent experiments. The continuous line represents a Hill equation (Eq. 3). D. *Reversibility of the PMCA inhibition by EGCG.* PMCA was preincubated with increasing concentrations of EGCG, PMCA/EGCG mixtures were diluted 10 times and PMCA activity was measured (○). As a control PMCA activity was measured in media with the same concentrations of EGCG as in the preincubation assay (●). Data are representative of two independent experiments. Measurements were carried out at 37 °C in the presence of 1.9 mM $[Mg^{2+}]_{free}$ and 80 μM $[Ca^{2+}]_{free}$. The reaction was started by the addition of 2 mM ATP. Results were related to PMCA activity measured in the absence of catechins (100%).

Table 1. Effect of catechins on PMCA activity. The table indicates the name and structure of each evaluated catechin and gallic acid, as well as the best fitting values of Ki (±standard error) obtained from data in Figures 2A, 2B and 2C.

Catechin	Structure	Ki (mM)
(−)-**Epicatechin** ((−)-cis-3,3′,4′,5,7-Pentahydroxyflavane)		>100
(+)-**Catechin** ((+)-trans-3,3′,4′,5,7-Pentahydroxyflavane)		66.6 ± 11.8
(−)-**Epigallocatechin gallate** ((−)-cis-3,3′,4′,5,5′,7-Hexahydroxy-flavane-3-gallate)		0.032 ± 0.003
Gallic acid		48.2 ± 1.6

The aim of this study was to investigate the effect of catechins on the activity of isolated PMCA and the mechanism through which EGCG inhibits PMCA activity in the isolated protein and in living cells. We found that EGCG was the most potent reversible inhibitor of isolated PMCA by stabilizing the E1P intermediate. EGCG also inhibited PMCA activity in the presence of CaM. Finally, studies in human embryonic kidney cells (HEK293T) that transiently overexpress hPMCA4 show that EGCG inhibited PMCA activity, suggesting that the effects observed on isolated PMCA could occur in living cells.

2. Materials and Methods

2.1. Chemicals

[γ-^{32}P]ATP was obtained from Perkin-ElmerNEN Life Sciences (USA). HEK293T cells were obtained from American Type Culture Collection (ATCC, Manassas, VA). Dulbecco's Modified Eagle's Medium (DMEM), fetal bovine serum (FBS), Lipofectamine LTX Reagent with PLUS Reagent and cell culture supplements were purchased from Invitrogen-Thermo Fisher Scientific (Carlsbad, CA, USA). Antibiotic/antimycotic solution was obtained from Life Technologies Inc. (Carlsbad, CA, USA). Fluo-4-AM probe was obtained from Molecular Probes (Eugene, OR, USA). PVDF blot membrane was obtained from BioRad Laboratories (Reinach, Switzerland). Dimyristoyl phosphatidylcholine (DMPC) was obtained from Avanti Lipids (Alabaster, AL, USA). Thapsigargin (TG),

(-)-epigallocatechin 3-gallate (EGCG), (-)-epicatechin, (+)-catechin, gallic acid, polyoxyethylene (10) lauryl ether ($C_{12}E_{10}$) and all the other chemicals used in this work were of analytical grade and were purchased from Sigma-Aldrich (St. Louis, MO, USA). Human blood recently drawn at Fundación Fundosol (Buenos Aires, Argentina) was used for the isolation of PMCA. Donors provided informed consent for the donation of blood and for its subsequent legitimate use by the transfusion service.

2.2. Purification of functional PMCA from human erythrocytes

A calmodulin (CaM) affinity chromatography column was used to isolate PMCA from CaM-depleted human erythrocyte membranes [23]. Briefly, 0.5% $C_{12}E_{10}$-containing buffer was used to solubilize membrane proteins, they were centrifuged, and the supernatants were loaded into a CaM-Sepharose column with 1 mM Ca^{2+}. The column was washed with a buffer containing 0.05% $C_{12}E_{10}$. PMCA was eluted in 20% (w/v) glycerol, 0.005% $C_{12}E_{10}$, 1 mM $MgCl_2$, 120 mM KCl, 2 mM EGTA, 10 mM MOPS-K (pH 7.4 at 4 °C) and 2 mM dithiothreitol. Isolated PMCA was assayed for protein concentration and homogeneity by SDS-PAGE (about 10 μg/ml, single band at Mr 134,000) and stored in liquid nitrogen. The purification procedure preserves transport activity, kinetic properties and regulatory characteristics of PMCA in its native milieu [24]. Human erythrocytes contain PMCA1 and PMCA4 isoforms. hPMCA4 is the predominant isoform expressed (80%) [25].
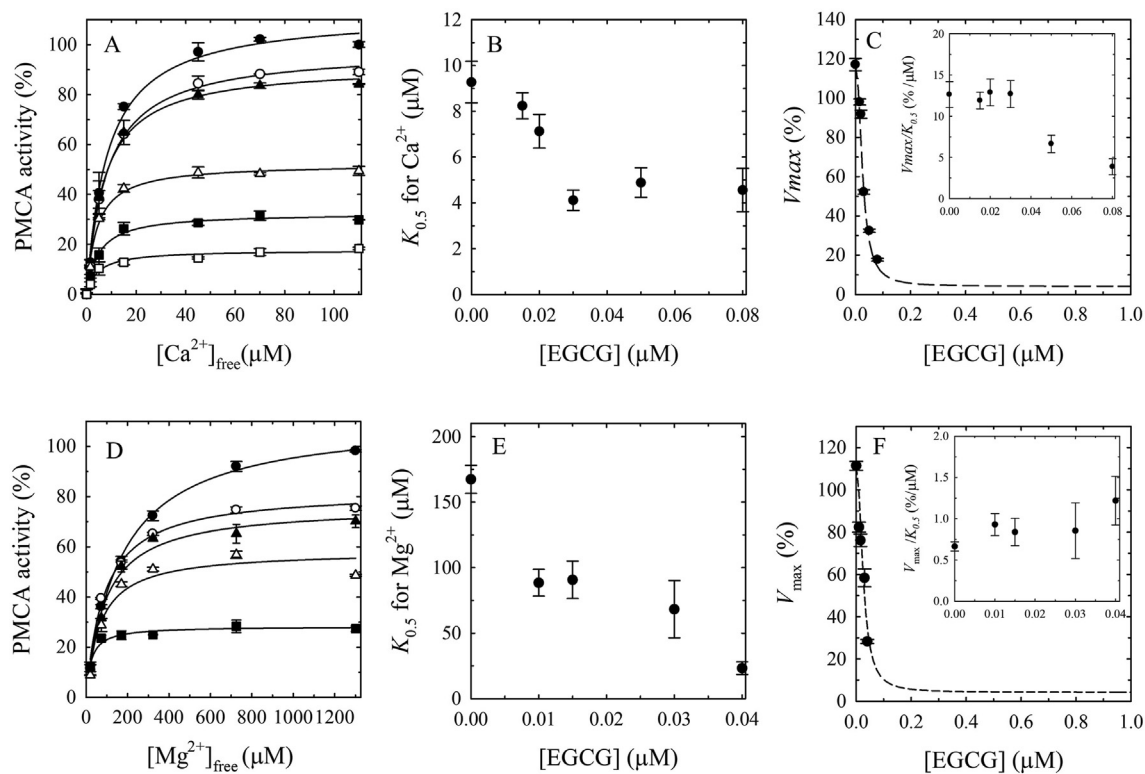
Figure 3. A-C. *Effect of Ca^{2+} on inhibition of PMCA activity by EGCG.* A. PMCA activity was measured at different Ca^{2+} concentrations in the presence of 0 (●); 0.015 (○); 0.02 (▲); 0.03 (△); 0.05 (■) and 0.08 (□) μM EGCG. Measurements were carried out at 37 °C in the presence of 1.9 mM $[Mg^{2+}]_{free}$ and the $CaCl_2$ required to obtain the $[Ca^{2+}]_{free}$ indicated in the abscissa axis. The reaction was started by the addition of 2 mM ATP. Data are expressed as the mean ± S.E. (n ≥ 3). The continuous lines represent rectangular hyperbolas (Eq. 4). Best fitting values of $K_{0.5}$ and V_{max} were obtained from Figure 3A. $K_{0.5}$ and V_{max} values were plotted as a function of EGCG concentrations (Panels B and C, respectively). Inset in C: $V_{max}/K_{0.5}$ ratio as a function of EGCG concentration. D-F. *Effect of Mg^{2+} on inhibition of PMCA activity by EGCG.* D. PMCA activity was measured at different Mg^{2+} concentrations in the presence of 0 (●), 0.015 (○), 0.02 (▲), 0.03 (△) and 0.04 (□) μM EGCG. Measurements were carried out at 37 °C in the presence of 80 μM $[Ca^{2+}]_{free}$ and the $MgCl_2$ required to obtain the $[Mg^{2+}]_{free}$ indicated in the abscissa axis. The reaction was started by the addition of 2 mM ATP. Data are expressed as the mean ± S.E. (n ≥ 3). The continuous lines represent rectangular hyperbolas (Eq. 4). Best fitting values of $K_{0.5}$ and V_{max} were obtained from Figure 3D. $K_{0.5}$ and V_{max} values were plotted as a function of EGCG concentrations (Panels E and F, respectively). Inset in F: $V_{max}/K_{0.5}$ ratio as a function of EGCG concentration.

2.3. Measurement of ATPase activity

PMCA ATPase activity assay was performed in the samples by measuring the $[^{32}P]Pi$ released from $[γ-^{32}P]ATP$ as described by Richards et al. [26] or alternatively performed according to the method of Fiske and Subbarow [27]. In both cases, PMCA was resuspended in micelles containing 80 μM $C_{12}E_{10}$ and 38 μM DMPC and PMCA activity was measured at 37 °C or 25 °C in media containing 30 mM MOPS (pH 7.4 at the indicated temperature), 120 mM KCl, and the necessary amount of $MgCl_2$ and $CaCl_2$ to obtain the desired final free cation concentration. The indicated catechin was added to the reaction medium in the presence of PMCA. The reaction was started by the addition of ATP (final concentration of 30 μM for radioactive assays and 2 mM for non-radioactive assays). Enzyme concentration was 0.8 μg/ml. The PMCA activity obtained at 80 μM free Ca^{2+} concentration was considered as 100%.

MaxChelator (https://somapp.ucdmc.ucdavis.edu/pharmacology/bers/maxchelator/downloads.htm) was used to estimate free Mg^{2+} and Ca^{2+} concentrations in the incubation media [28]. The free Mg^{2+} and Ca^{2+} concentrations and some components varied according to the experiments and are indicated in the figure legends.

2.4. Determination of phosphorylated intermediates

Phosphorylated intermediates (*E*P) were measured as the amount of acid-stable ^{32}P incorporated into the enzyme from $[γ-^{32}P]ATP$ after stopping the reaction with an ice-cold solution containing 10%

trichloroacetic acid. The determination of *E*P was performed at 25 °C or 0 °C in 30 mM MOPS (pH 7.4 at the indicated temperature), 120 mM KCl, 2 mM $MgCl_2$ (final free Mg^{2+} concentration of 1.9 mM), 80 μM $C_{12}E_{10}$, 38 μM PC, 30 μM ATP, and the necessary amount of $CaCl_2$ required to obtain the final free Ca^{2+} concentration of 80 μM. EGCG was added to the reaction medium in the presence of PMCA and the reaction was then initiated by adding $[γ-^{32}P]ATP$. The isolation and quantification of *E*P was performed according to Echarte et al. [29].

2.5. ADP-dependent dephosphorylation

ADP-dependent dephosphorylation was performed as previously described [30, 31]. The isolated PMCA was phosphorylated for 3 min at 0 °C in 30 mM MOPS (pH 7.4 at 0 °C), 120 mM KCl, 2 mM $MgCl_2$ (final free Mg^{2+} concentration of 1.9 mM), 80 μM $C_{12}E_{10}$, 38 μM PC, 30 μM $[γ-^{32}P]ATP$, and the necessary amount of $CaCl_2$ required to obtained the final free Ca^{2+} concentration of 80 μM in the presence of 0 or 5 μM EGCG. Dephosphorylation was initiated by adding a chase solution yielding final concentrations of 2 mM ADP and 30 μM unlabeled ATP followed by acid quenching at different time intervals. The isolation and quantification of *E*P was performed according to Echarte et al. [29].

2.6. Data analysis

Theoretical equations were fitted to experimental data by nonlinear regression based on the Gauss-Newton algorithm using commercial
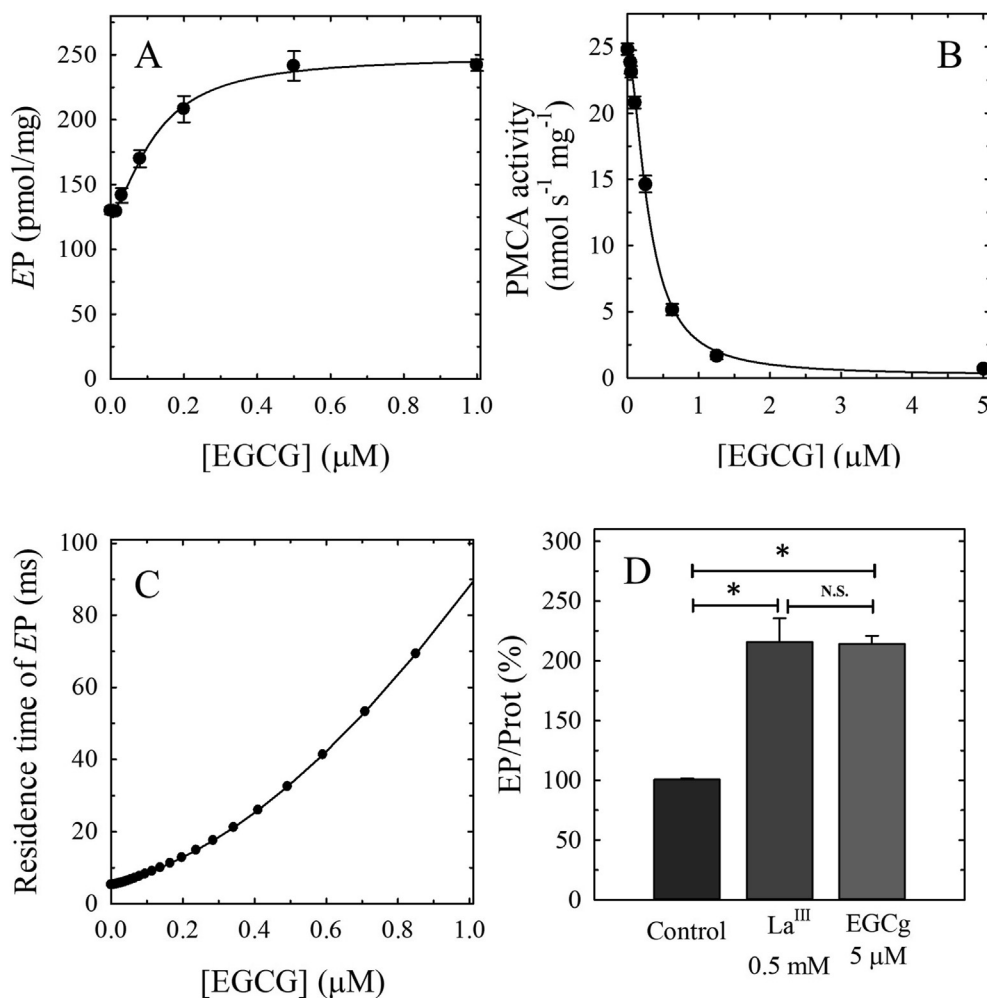
Figure 4. Effect of EGCG on PMCA phosphorylated intermediate (EP). A. PMCA phosphorylated intermediate levels were measured in the presence of increasing amounts of EGCG. Measurements were carried out at 25 °C for 30 s (steady state) in the presence of 1.9 mM $[Mg^{2+}]_{free}$, 80 μM $[Ca^{2+}]_{free}$ and increasing amounts of EGCG. The reaction was started by the addition of 30 μM $[\gamma^{32}$-P]ATP. The continuous line represents a Hill equation (Eq. 5). B. PMCA activity measurements were carried out in the same conditions as PMCA phosphorylation measurements. The continuous line represents a Hill equation (Eq. 3). Data are expressed as the mean ± S.E. (n ≥ 3). C. Residence time of EP as a function of [EGCG]. Residence time of EP was calculated as the ratio between the EP levels and PMCA activity (from the fitting curves in A and B, respectively). D. EP levels in steady state in the absence (control) or in the presence of 500 μM La^{III} or 5 μM EGCG. The EP level obtained for control was established as 100%. Data are expressed as the mean ± S.E. (n ≥ 3). EP levels significantly different from controls (*p > 0.01; one-way ANOVA with Bonferroni post-tests). N.S.: Non-significant.

Table 2. Best fitting values (±standard error) of E1P and E2P and the E1P/E2P ratio obtained from data in Figure 5.

Condition	E1P (%)	E2P (%)	E1P/E2P
Control	35.3 ± 5.9	64.7 ± 4.9	0.55 ± 0.13
EGCG 5 μM	188.0 ± 0.4 ***	41.4 ± 0.4**	4.55 ± 0.05***

Significant differences from control (**p < 0.001, ***p < 0.0001, Student's t-test).

programs (Excel and Sigma-Plot for Windows, the latter being able to provide not only the best fitting values of the parameters but also their standard errors). The goodness of fit of a given equation to the experimental results was evaluated by the corrected AIC criterion (AIC$_C$) defined as:

$$AIC_C = N \ln(SS/N) + 2PN/(N- P-1) \qquad \text{Eq.1}$$

where N is the number of data, P is the number of parameters plus one, and SS is the sum of weighted square residual errors [32]. Unitary weights were considered in all cases and the best equation was chosen as that giving the lower value of AIC$_C$. The AIC criterion is based on Information Theory, and selects an equation among several possible equations based on its capacity to explain the results using a minimal number of parameters. Parameter values are expressed as the mean ± standard error (S.E.).

Eq. (2) was fitted to the experimental data from PMCA activity vs [(-)-epicatechin] or [(+)-catechin] (section 3.1), which were described by a decreasing rectangular hyperbola.

$$v = \frac{Vmax\ K_i}{K_i + [Catechin]} \qquad \text{Eq. 2}$$

where $Vmax$ is the PMCA activity when the catechin concentration ([(-)-epicatechin] or [(+)-catechin]) tends to 0, and K_i represents the catechin concentration ([(-)-epicatechin] or [(+)-catechin]) at which the half-maximum effect is achieved.

Eq. (3) was fitted to the experimental data from PMCA activity vs [ligand] ([EGCG] or [Acid gallic]) (section 3.1), which were described by a Hill equation:

$$v = V_{min} + \frac{(V_{max} - V_{min})}{1 + \left(\frac{[Ligand]}{K_i}\right)^n} \qquad \text{Eq. 3}$$

where $Vmax$ is the PMCA activity when the EGCG concentration tends to zero, $Vmin$ is the PMCA activity when the EGCG concentration tends to infinity, "n" is the Hill coefficient and K_i represents the EGCG concentration at which the half-maximum effect is achieved.
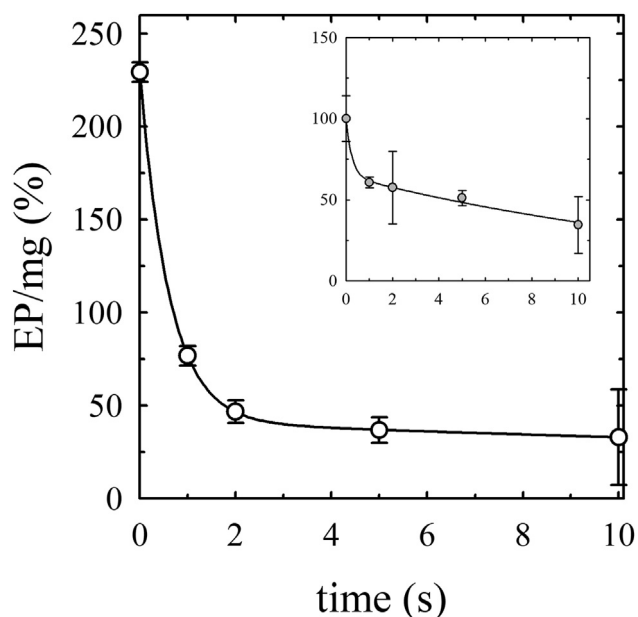
Figure 5. Time course of ADP-dependent dephosphorylation. PMCA phosphorylation measurements were carried out at 0 °C in the presence of 1.9 mM $[Mg^{2+}]_{free}$, 80 µM $[Ca^{2+}]_{free}$ and 5 µM EGCG or in the absence of EGCG (*inset*). The reaction was started by the addition of 30 µM $[\gamma^{32}-P]$ATP. After 3 min of reaction, when the phosphorylated intermediates reached a steady-state level, dephosphorylation was initiated by adding a chase solution yielding final concentrations of 2 mM ADP and 30 µM unlabeled ATP followed by acid quenching solution at different time intervals. Data are expressed as the mean ± S.E. (n = 3) and are shown as a percentage of the steady-state *E*P level obtained after 3 min of phosphorylation (100%). The continuous line represents a bi-exponential time function (Eq. 7). The best fitting values for *E*1P and *E*2P are shown in Table 2.

Eq. (4) was fitted to the experimental data from PMCA activity vs [Cation] (section 3.2), which were described by the rectangular hyperbola:

$$v = \frac{Vmax \ [Cation]}{K_{0.5} + [Cation]} \qquad \text{Eq. 4}$$

where *Vmax* is the PMCA activity when the cation concentration ($[Ca^{2+}]$ or $[Mg^{2+}]$) tends to infinity, and $K_{0.5}$ represents the [Cation] ($[Ca^{2+}]$ or $[Mg^{2+}]$) at which the half-maximum effect is achieved.

Eq. (5) was fitted to the experimental data from *E*P vs [EGCG] (section 3.2), which were described by following Hill equation:

$$EP = EP_0 + \frac{(EP_{max} - EP_0)[EGCG]^n}{K_{0.5}{}^n + [EGCG]^n} \qquad \text{Eq. 5}$$

where EP_0 and EP_{max} are the amounts of PMCA phosphorylated in the absence of EGCG and in the presence of non-limiting concentrations of the inhibitor, respectively, "n" is the Hill coefficient, and $K_{0.5}$ is the concentration of EGCG at which $EP = (EP_{max} + EP_0)/2$.

One-way analysis of variance (ANOVA) followed by Bonferroni post-test and Student's t-test were performed using GraphPad Prism version 6.00 for Windows, GraphPad Software (San Diego, CA, USA). A probability (P) value <0.05 was considered statistically significant. The number of independent experiments (n) is indicated in each figure legend.

2.7. Docking experiments

The homology model of PMCA4 was obtained using Modeller 9.22 [33]. A homology model of hPMCA4b was made using human PMCA isoform 1 (hPMCA1) structure [34] as template (PDB ID: 6A69).

Phospholipid binding domain (294-349) and C-terminal (1076-1241) were not included in the model (these sections are not defined in the template). Template and PMCA4b sequences were aligned using Modeller alignment algorithm. Protein and ligand structures were prepared using AutoDock Tools [35]. The grid box was set to include all the cytoplasmic domains of PMCA and more than 50 trials were conducted for each ligand using AutoDock Vina [36]. The lowest energy conformations were regarded as the best binding conformations of each flavonoid. Visualization was performed using Chimera [37].

2.8. Cell culture and overexpression of hPMCA4

HEK293T cells were cultured as monolayers in Dulbecco's Modified Eagle's Medium (DMEM) supplemented with 10% (v/v) FBS and 1% (v/v) antibiotic/antimycotic solution at 37 °C in a 5% CO_2 atmosphere. Cells were transfected with EGFP-hPMCA4b plasmid [38] using Lipofectamine LTX with Plus Reagent as described in the manufacturer's protocol (Thermo-Fisher Scientific). HEK293T-mock cells (cells transfected with the empty vector) were cultured in parallel as control of expression and activity. hPMCA4 overexpression was verified by Western blot.

2.9. Dynamics of cytoplasmic Ca^{2+} measurements

HEK293T cells were seeded on sterile 96-well black-walled, clear-bottom plates (Corning Inc., Corning, NY, USA) at a density of 1.5×10^4 cells/well. After 18 h, cells were transfected with mock or EGFP-hPMCA4b plasmid, and the dynamics of $[Ca^{2+}]_{CYT}$ was assayed 18 h after transfection using Fluo4-AM. Cells were loaded for 1 h at 37 °C with 5 µM of the fluorophore in reaction buffer (RB) composed of 10 mM Hepes (pH 7.4 at 37 °C), 120 mM choline chloride, 5 mM KCl, 1 mM $MgCl_2$ and 5 mM D-glucose. This buffer contained choline chloride instead of NaCl to minimize the effect of the Na^+/Ca^{2+} exchanger. After dye loading, the plates were washed twice and 100 µl of RB was added to the samples. Cells were then incubated with EGCG or RB for 30 min. The EGCG concentration used was the maximum at which cells maintained their adherence and shape. Fluorescence was measured at λ excitation 485 ± 20 nm (λ emission: 528 ± 20 nm) in a fluorometric plate reader (Synergy HT. Biotek, BioTek Instruments Inc., Winooski, VT, USA). Fluorescence signals were analyzed using software Gen 5.2.01. Stable baseline values were established for at least 3 min then 2 µM TG was added and the fluorescence was recorded for at least 5 min. TG specifically inhibits SERCA, which induces depletion of ER Ca^{2+} stores leading to a rise in intracellular Ca^{2+} [39]. Traces showing the time course of fluorescence intensity were normalized to the baseline and expressed as relative $[Ca^{2+}]_{CYT}$. EGCG did not interfere with FLUO4 fluorescence (data not shown). The area under the curve (AUC) is the integral of $[Ca^{2+}]_{CYT}$ from TG addition until basal levels are reached or until the end of measurements. Activity of hPMCA4 was calculated using the AUCs and Eq. (6), as described by Dalghi et al. [40].

$$hPMCA4 \, activity(\%) = \frac{(AUC_{mock,treatment} - AUC_{PMCA4,treatment})}{(AUC_{mock.control} - AUC_{PMCA4,control})} \times 100 \qquad \text{Eq. 6}$$

2.10. Detection of PMCA expression in HEK293T cells

The collected cells were directly solubilized in sample buffer containing 150 mM Tris-HCl (pH 6.8), 4 % SDS, 5% DTT, 20% glycerol, urea (125 mg/ml) and bromophenol blue. The ladder was Precision Plus Protein™ Dual Color Standards (BioRad). Samples were separated using a 10% SDS gel (50 µg protein per lane), and proteins were transferred to a PVDF blot membrane (BioRad). After blocking, the blot was incubated with the anti-PMCA primary mouse monoclonal antibody 5F10 [41] (1:2000; Pierce) or anti-GADPH (1:1000, Cell signaling) overnight at 4 °C. Anti-mouse IgG, horseradish peroxidase-linked whole antibody (1:20000; Amersham, Buckinghamshire, UK) or anti-rabbit IgG, horseradish peroxidase-linked whole antibody (1:1000; Amersham,
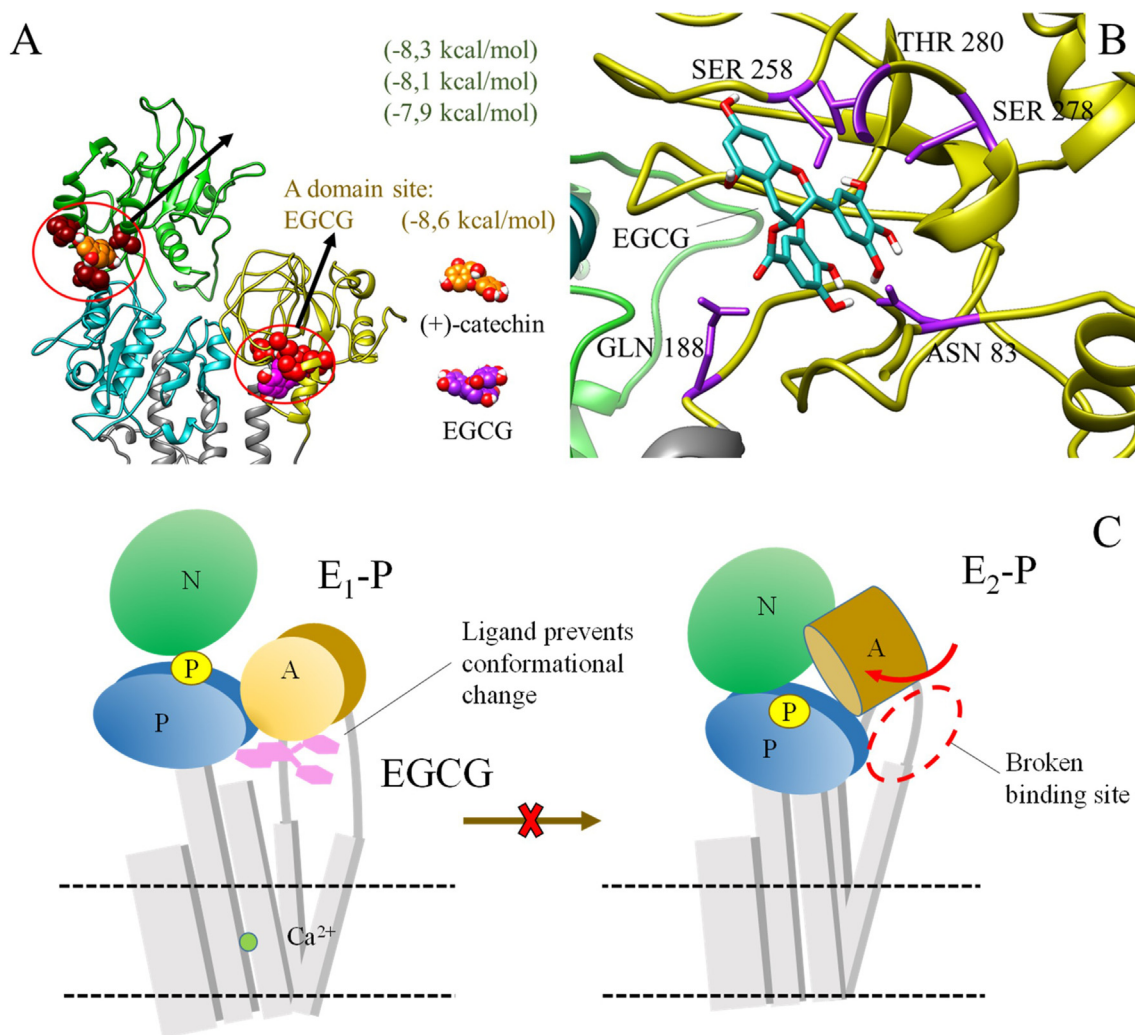
Figure 6. Docking experiments on the hPMCA4 structure. A. The cytoplasmic domains of PMCA are depicted, the N-domain in green, the A-domain in yellow, the P domain in blue and the transmembrane domain in grey. Two binding sites were found for EGCG, one in the A-domain with higher binding energy, and the other in the N-domain with lower binding energy as shown in the figure. The N-domain binding site was also the binding site for (+)-catechin and (-)-epicatechin ((+)-catechin is shown in the site). B. The binding conformation of EGCG in the A-domain is shown. The PMCA amino acids that form hydrogen bonds with the ligand are depicted. C. The scheme shows the proposed binding mechanism of EGCG based on the kinetic data and docking simulations.

Buckinghamshire, UK) were used as the secondary antibody. Immunoreactive bands were visualized using the enhanced chemiluminescence method (Kalium Technologies, Buenos Aires, Argentina). Digital images were quantified using GelPro Analyzer version 4.0. Protein density was normalized to the GAPDH loading control.

3. Results and discussion

3.1. Effect of catechins on PMCA activity

The effects of three catechins on PMCA activity were evaluated using isolated PMCA from human erythrocytes. Figures 2A and 2B show PMCA activity measured in the presence of different concentrations of (-)-epicatechin, (+)-catechin (Figure 2A) and EGCG (Figure 2B). The best fitting values of the apparent constant of inhibition (K_i) are shown in Table 1. Results indicate that the three catechins affected PMCA activity; however, EGCG induced a strong inhibition of PMCA activity. Studies with Na$^+$/K$^+$-ATPase have shown that EGCG is a potent inhibitor of ATPase activity with a K_i of 1 µM [21].

Since one of the structural differences between (-)-epicatechin and EGCG is the gallate group, the effect of gallic acid on PMCA activity was studied. Figure 2C shows that gallic acid inhibited PMCA activity with a low apparent affinity ($K_i = 48.2 \pm 1.6$ µM), suggesting that the flavonoid base structure is necessary for the strong inhibition by EGCG and therefore, the gallate ring structure alone could not be responsible for the effects of EGCG on PMCA.

Next, the reversibility of PMCA inhibition by EGCG was evaluated (Figure 2D). Results show that upon a ten-fold dilution of EGCG, PMCA activity tended to recover the original values, indicating that EGCG is a reversible inhibitor.

Recently, we studied the inhibitory effect of flavonoids on PMCA activity and we demonstrated that the presence of a double bond between C2-C3 and the hydroxylations in the B ring were critical for flavonoids to inhibit PMCA activity (i.e. quercetin and gossypin) [17]. Catechins do not have a keto group or a double bond between C2-C3; then, C2 and C3 are two chiral centers that generate different configurations. The two isomers, (-)-epicatechin (cis configuration) and (+)-catechin (trans configuration), showed differences as PMCA activity inhibitors, with the former showing less affinity. Therefore, the configuration of catechins would be important for the inhibition of PMCA activity, in particular, the orientation of –OH in C3. On the other hand, EGCG (the most potent catechin) has the same configuration as (-)-epicatechin (less active catechin), but EGCG has a gallic acid conjugated in C3 and one more –OH group in the B ring. Results obtained with gallic
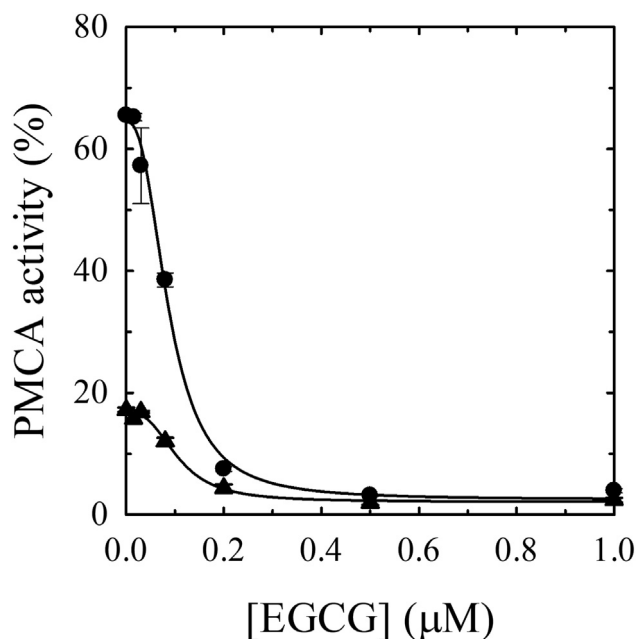
Figure 7. Effect of different concentrations of EGCG on PMCA activity in presence of CaM. PMCA activity was measured as a function of EGCG concentrations in the absence (▲) or in the presence of 120 nM CaM (●). Measurements were carried out at 37 °C in the presence of 1.9 mM $[Mg^{2+}]_{free}$ and 2 μM $[Ca^{2+}]_{free}$. The reaction was started by the addition of 2 mM ATP. Results are expressed as the percent of PMCA activity measured in the absence of EGCG and 80 μM $[Ca^{2+}]_{free}$ (100%). The continuous lines represent a Hill equation (Eq. 3). Data are expressed as the mean ± S.E. (n = 3).

acid (Figure 2C) indicated that the flavonoid base structure, including the galloyl group at the 3 position, is necessary for the strong inhibition showed by EGCG. This is consistent with previous findings that suggested that the galloyl group is relevant in the specificity of the binding of catechins to proteins [42, 43].

3.2. Effect of Ca^{2+} and Mg^{2+} on PMCA inhibition

The isolated PMCA activity was measured as a function of Ca^{2+} or Mg^{2+} concentration in the presence of different concentrations of EGCG (Figures 3A and 3D, respectively). In both cases, experimental data were described by a rectangular hyperbola (Eq. 4). The best fitting values of $K_{0.5}$ for Ca^{2+} and *Vmax* were plotted as a function of EGCG concentrations (Figures 3B and 3C, respectively). Results show that increasing EGCG concentrations up to 0.03 μM decreased $K_{0.5}$ values for Ca^{2+}, whereas higher concentrations of the inhibitor did not produce significant changes. Also, *Vmax* decreased as a function of EGCG concentration. The ratio between *Vmax* and $K_{0.5}$ for Ca^{2+} did not change up to 0.03 μM EGCG but decreased at higher EGCG concentrations (*inset* Figure 3C). These results suggest that, with respect to Ca^{2+}, EGCG may be an uncompetitive inhibitor at low concentrations (up to 0.03 μM) and a noncompetitive inhibitor at higher concentrations.

The best fitting values of $K_{0.5}$ for Mg^{2+} and *Vmax* were plotted as a function of EGCG concentration (Figures 3E and 3F, respectively). Results show that both $K_{0.5}$ for Mg^{2+} and *Vmax* decreased as a function of EGCG concentration, leaving the ratio between *Vmax* and $K_{0.5}$ unchanged (*inset* Figure 3F). These results suggest that EGCG is an uncompetitive inhibitor with respect to Mg^{2+}.

Our results demonstrate that EGCG was a reversible inhibitor of PMCA and did not compete with Ca^{2+} or Mg^{2+}, suggesting that EGCG does not prevent the binding of these cations to PMCA. These results also suggest that the EGCG binding site is different from those of Ca^{2+} or Mg^{2+}. On the other hand, Soler et al. [22] have shown that EGCG inhibits

Ca^{2+} binding to SERCA and proposed a binding site in its transmembrane region near the cytoplasmic surface.

3.3. Effect of EGCG on steady state levels of phosphorylated intermediates

To gain insight into the inhibition mechanism and the ATP interaction with PMCA, we evaluated the effect of EGCG on phosphorylated intermediates. *E*P levels were measured as a function of EGCG concentration (Figure 4A).

Results show that *E*P levels increased with EGCG concentration and the data were described by a Hill equation (Eq. 5). The best fitting values for EP_0, EP_{max} and $K_{0.5}$ were 128.0 ± 2.4 pmol/mg; 249.0 ± 8.2 pmol/mg and 0.12 ± 0.01 μM, respectively. In parallel experiments, PMCA activity was measured as a function of EGCG concentration under the same conditions as for the *E*P measurements (Figure 4B). The best fitting value obtained for *Ki* was 0.29 ± 0.02 μM (Eq. 3), which was similar to that obtained from the *E*P measurements.

The residence time of *E*P was calculated as the ratio between the *E*P levels and PMCA activity (Figure 4C) at the same EGCG concentration. Residence time is the mathematical inverse of the turnover. The residence time of *E*P indicates the average time spent by the enzyme in the phosphorylated states. This figure shows that the residence time of *E*P increased as a function of EGCG concentration, suggesting that the *E*P breakdown rate is concomitantly decreased.

The effects of EGCG on PMCA phosphorylation were further studied by comparing the steady-state levels of *E*P in the absence (control) or in the presence of 5 μM EGCG or 500 μM $LaCl_3$ (Figure 4D). La^{III} inhibits PMCA activity by producing an accumulation of $E1P$ [20, 44]. The *E*P level obtained for control was established as 100%. Our results show that, in the presence of EGCG, hPMCA4 was phosphorylated at the same level as in the presence of La^{III} in conditions where the inhibition of PMCA activity was maximal (Figure 4D).

Our results suggest that EGCG produced an increase in *E*P levels by a decrease in the rate of *E*P breakdown rather than an increase in the phosphorylation rate. Therefore, EGCG interacts with phosphorylated conformations ($E1P$ and/or $E2P$) and prevents hPMCA4 dephosphorylation.

As EGCG increases *E*P levels, it did not compete with ATP binding. Further, the *K*i values obtained for ATPase activity determinations using 2 mM and 30 μM ATP were 0.032 ± 0.003 μM and 0.29 ± 0.02 μM, respectively, suggesting that EGCG may be an uncompetitive inhibitor with respect to ATP. Since EGCG does not prevent the binding of ATP it is possible that EGCG binds to a different site, but we cannot rule out that EGCG interacts with hPMCA4 through the nucleotide binding site after PMCA is phosphorylated by ATP because phosphorylated conformations contain that site.

3.4. ADP sensitivity of the phosphoenzyme

To evaluate the effect of EGCG on the distribution of the phosphoenzyme between $E1P$ and $E2P$, the time course of ADP-sensitive dephosphorylation was studied. Since $E1P$ can donate a phosphoryl group back to ADP forming ATP, $E1P$ is dephosphorylated rapidly by ADP. However, $E2P$ is ADP-insensitive and it is dephosphorylated very slowly by ADP. The time course of dephosphorylation by ADP could be described by a bi-exponential function of time, where the rapid and slow components reflect the amounts of ADP-sensitive $E1P$ and ADP-insensitive $E2P$, respectively. Figure 5 shows the time course of dephosphorylation initiated by addition of 2 mM ADP and 30 μM unlabeled ATP to the phosphoenzyme formed previously in the presence of 30 μM [γ-^{32}P]ATP and 5 μM EGCG or without EGCG (Figure 5, *inset*). For both conditions, the time course of *E*P can be described by:

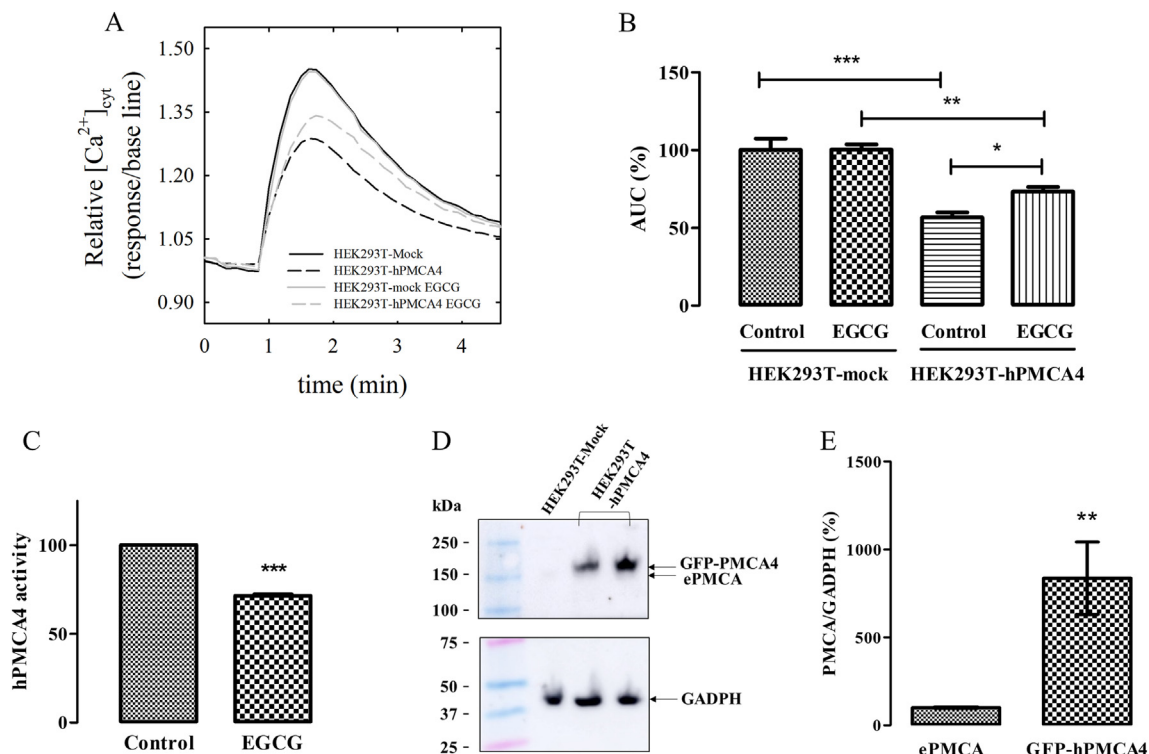$$\%EP = E1Pe^{-k_1 t} + E2Pe^{-k_2 t} \qquad \text{Eq. 7}$$

Figure 8. Effect of EGCG on hPMCA4 overexpressed in HeK293T. A. Continuous lines correspond to the time course of $[Ca^{2+}]_{CYT}$ in HEK293T-mock cells in the presence (grey line) or in the absence (black line) of EGCG (50 μM) upon addition of TG (2 μM). Dotted lines correspond to representative traces of the time course of $[Ca^{2+}]_{CYT}$ in HEK293T-hPMCA4 cells in the presence (grey line) or in the absence (black line) of EGCG (50 μM) upon addition of TG (2 μM). The curves are representative of three independent experiments performed with n = 6. B. AUC of $[Ca^{2+}]_{CYT}$ signal after TG (2 μM) addition for the conditions assayed. AUC were calculated from data obtained in A. Significant differences from controls (*p < 0.05, **p < 0.01, ***p < 0.001, one-way ANOVA). C. Effect of EGCG on hPMCA4 activity in HEK293T cells. Activity value was obtained from data from B as described in Materials and Methods. Data shown are mean ± S.E. Significant differences from control (***p < 0.001, Student's t-test). D. Immunoblot of total PMCA protein expression in whole lysate using the 5F10 antibody. Image is representative from four independent experiments. GAPDH was used as a loading control (from Figure S1). E. PMCA expression from densitometric analysis normalized to the GADPH loading control. Data shown are mean ± S.E (n > 3). The PMCA value obtained for HEK293T-mock cells was established as 100%. Significant differences from control (**p < 0.01, Student's t-test). ePMCA, endogenous PMCA in HEK293T cells; GFP-hPMCA4, PMCA overexpressed in HEK293T cells transfected with EGFP-hPMCA4b plasmid (HEK293T-hPMCA4 cells).

where $E1P$ and $E2P$ are the amounts of the ADP-sensitive and ADP-insensitive phosphoenzyme, respectively; t is the time and k_1 and k_2 are rate coefficients. The best fitting values of $E1P$ and $E2P$ were obtained for both conditions and the $E1P/E2P$ ratio was calculated (Table 2).

Our results indicated that the time courses of EP dephosphorylation by ADP in the absence or in the presence of EGCG show a biphasic behavior indicating that EP levels are composed of both $E1P$ and $E2P$ conformations (Figure 5). In the presence of EGCG, the ratio $E1P/E2P$ was about eight-fold higher than in the control suggesting that EGCG favors $E1P$ in the distribution between phosphoenzyme intermediates (Table 2). This is in agreement with results obtained in Na^+/K^+-ATPase, which showed that EGCG reduces the $E1P$ to $E2P$ transition rate, thus favoring the $E1P$ conformation [21]. However, in SERCA, EGCG induces the stabilization of a Ca^{2+}-free state as $E2$ [22]. In this context, PMCA seems to behave as the Na^+/K^+-ATPase rather than as SERCA.

3.5. Docking simulations

Our experimental results indicate that EGCG is an uncompetitive inhibitor with respect to Mg^{2+}, Ca^{2+} (at EGCG concentrations lower than 0.03 μM) and ATP. Therefore, the binding site of the inhibitor would be different from the binding site of these substrates and cofactor. To gain insight into the binding site of EGCG in PMCA, we performed docking simulations on a PMCA4b homology model based on the structure of PMCA1 in $E1$ conformation [34]. EGCG,

(-)-epicatechin and (+)-catechin were docked using a box that included the cytoplasmic domains of PMCA. Our results indicate that EGCG binding site would bind with higher affinity (-8,6 kcal/mol) to a site located in the A-domain of the protein and with lower affinity (-8,3 kcal/mol) to a site located in the N-domain near the ATP binding site. In contrast (-)-epicatechin and (+)-catechin would bind only to the N-domain, at the same site that EGCG (Figure 6A and B). The binding of EGCG to the A-domain would agree with our experimental data as the flavonoid would not compete with the binding of substrates and cofactors, allowing the pump to phosphorylate. Moreover, the presence of EGCG in the binding site suggested by our simulations would hamper the rotation of the A-domain which is critical for the $E1P$ to $E2P$ transition in P-type ATPases (Figure 6C) [45, 46]. On the other hand, the binding of EGCG to the N-domain near the ATP binding site was also evaluated since EGCG would be near the phosphorylation site and EGCG interacts with phosphate groups [47, 48]. However, EGCG binding to this site would not explain why EGCG blocks the PMCA reaction cycle in $E1P$, making it less likely of being responsible for PMCA Ca^{2+}-ATPase activity inhibition at low EGCG concentrations. The binding of (-)-epicatechin and (+)-catechin in the N-domain agrees with this hypothesis as these inhibitors have a Ki at least three orders of magnitude higher than that of EGCG. Therefore, our docking simulations indicate that it is possible for EGCG to bind to a different site from the ATP, Ca^{2+} or Mg^{2+} binding sites and that the binding of the ligand would hamper the conformational change $E1P$ to $E2P$, stabilizing the phosphorylated intermediate.

3.6. Effect of EGCG on PMCA activation by calmodulin

PMCA activity was measured as a function of EGCG concentration in the presence of CaM (Figure 7). Results show that PMCA activity in the presence of CaM was inhibited by EGCG with an affinity ($K_i = 0.087 \pm 0.007\ \mu M$) that was similar to that found in the absence of CaM ($K_i = 0.10 \pm 0.01\ \mu M$). Note that the differences observed between these values of K_i and the value of K_i for EGCG previously reported (section "*Effect of catechins on PMCA activity*") may be due to the different Ca^{2+} concentration used in the activity determination.

PMCA is highly regulated by CaM. When cytoplasmic Ca^{2+} increases, CaM binds to the auto-inhibitory region of PMCA, inducing a conformational change from an inhibited state to an activated one [49, 50]. PMCA activity inhibition by EGCG occurred in the absence and in the presence of CaM with similar apparent affinities, indicating that EGCG does not interact with the CaM binding site. This evidence is relevant because the CaM-activated PMCA is in charge of expelling Ca^{2+} during a transient increase of the concentration of this cation in the cytoplasm of living cells.

3.7. Effect of EGCG on the dynamics of cytoplasmic Ca^{2+} in HEK293T cells

To assess whether the effects of EGCG observed on the isolated hPMCA4 could occur in living cells, the dynamics of $[Ca^{2+}]_{CYT}$ was studied in HEK293T cells overexpressing hPMCA4 according to the method previously described [17, 40].

Certain stimuli in the cells induce an increase of $[Ca^{2+}]_{CYT}$ levels, from intracellular stores or from the extracellular medium, which must be restored to basal stationary $[Ca^{2+}]_{CYT}$ levels. The increase in cytoplasmic Ca^{2+} is removed by the Na^+/Ca^{2+} exchanger and the PMCA, exported into the ER through the SERCA, into the mitochondria and chelated by cytosolic proteins [51]. As we previously described [17], to enhance the role of PMCA in Ca^{2+} extrusion, the Na^+/Ca^{2+} exchanger activity was minimized avoiding the presence of Na^+ in the extracellular media, whereas SERCA activity was inhibited using TG. As PMCA does not have specific inhibitors and different mechanisms can produce Ca^{2+} extrusion under the experimental conditions, we overexpressed hPMCA4 in the HEK293T cell line and evaluated the effect of EGCG.

The dynamics of $[Ca^{2+}]_{CYT}$ was examined by studying the changes in $[Ca^{2+}]_{CYT}$ generated by Ca^{2+} release from the ER upon the addition of TG, a SERCA inhibitor that induces a transient elevation in $[Ca^{2+}]_{CYT}$. Following $[Ca^{2+}]_{CYT}$ elevation, there is a recovery phase where Ca^{2+} is removed from cytoplasm and restored to basal levels.

The dynamics of $[Ca^{2+}]_{CYT}$ was evaluated in HEK293T-mock and HEK293T-hPMCA4 cells treated with and without 50 μM EGCG for 30 min (Figure 8A). This EGCG concentration, approximately three orders of magnitude higher than the K_i value obtained in the assays with the purified enzyme, was necessary to maximize the effects observed in the cells. Thus, it is likely that the high affinity of PMCA inhibition for EGCG observed in vitro is offset by the low availability of the inhibitor within the cell.

The effect on the dynamics of $[Ca^{2+}]_{CYT}$ was quantified as the AUC representing the overall excess of $[Ca^{2+}]_{CYT}$ relative to its basal level during the transient change. Provided that the Ca^{2+} uptake is not affected by a ligand; AUC will provide a measure of the ligand effect on the extrusion mechanism. The AUC values obtained were analyzed for HEK293T-mock and HEK293T-hPMCA4 cells in the absence and in the presence of EGCG (Figure 8B). The AUC value obtained for HEK293T-mock cells in the absence of EGCG was established as 100%. Results show that the AUC value obtained in the absence of EGCG was lower when cells overexpressed hPMCA4, suggesting that the Ca^{2+} extrusion mechanism was more effective in HEK293T-hPMCA4 cells. Figures 8D and 8E show hPMCA4 overexpression by Western blot and its quantification, respectively. Results indicate that hPMCA4 overexpression was about 8-fold higher in HEK293T-hPMCA4 cells; therefore, a significantly

enhanced Ca^{2+} extrusion in these cells can be explained by the presence of more enzyme units. This enhanced Ca^{2+} extrusion was also found by other authors when different isoforms were overexpressed [17, 40, 52, 53].

Treatment with EGCG on HEK293T-mock cells showed no significant effect (~AUC values, Figure 8B), which indicates that, in these experimental conditions, Ca^{2+} release from the ER and Ca^{2+} removal from the cytosol remained unaltered. Thus, the endogenous transport systems involved in these processes were not affected by EGCG (~AUC values). We obtained similar results for flavonoids quercetin and gossypin [17]. Treatment with EGCG on HEK293T-hPMCA4 cells induced an increase in the AUC value suggesting that the Ca^{2+} extrusion mechanism was less effective in the presence of EGCG.

The contribution of hPMCA4 overexpression to the effect of EGCG on the hPMCA4 activity was calculated using Eq. (6) (Figure 8C). Results show that the treatment with EGCG significantly decreased hPMCA4 activity. Our findings suggest that EGCG inhibition of PMCA activity observed in isolated PMCA may occur in living cells.

Our hypothesis proposes that the EGCG binding site in PMCA is in cytoplasmic domains, for this process to occur, EGCG should be able to enter the cells. Several studies have reported that EGCG enters the cell by diffusion [54, 55] or by certain transporters in intestinal cells [56]. Additionally, EGCG was found in the cytoplasm of the cells after incubations of minutes [54]. Based on these findings, we assumed that, in our experimental conditions, EGCG enters HEK293T cells and interacts with cytoplasmic domains of hPMCA4. However, considering the complexity of cellular systems, other underlying mechanisms cannot be ruled out.

Alterations of Ca^{2+} signaling can be a characteristic of certain pathologies [57, 58, 59, 60]. Cancer has been associated with malfunctions of Ca^{2+} signaling which may be significant and contribute to tumor progression. Changes in the expression levels of proteins that regulate cytoplasmic free Ca^{2+} concentrations were shown to be responsible for the alterations of Ca^{2+} signaling in cancer cells [61, 62]. Numerous studies have reported alterations of PMCA expression in some pathological cells [59, 63, 64, 65, 66]. PMCA4 isoform is down-regulated in human colon cancer cell lines and increases its expression with cell differentiation [64, 66]. On the other hand, PMCA2 isoform is overexpressed in some breast cancer cell lines [63, 67, 68] and in clinical human samples [69]. The increase of PMCA expression may be associated with alterations of Ca^{2+} efflux that contributes to the acquisition of an anti-apoptotic phenotype in the cancer cells [64, 68, 70]. The study of the role of PMCA in Ca^{2+} signaling and cancer processes involves finding pump inhibitors/activators as an alternative to genetic approaches. In this sense, our findings might be a relevant contribution to this field. Since our results indicate that the effect of EGCG is only observed when cells overexpress hPMCA4 and considering that PMCA overexpression has been observed in several tumor cells, further research should be oriented to study the effect of EGCG on these cells to characterize the role of PMCA in Ca^{2+} signaling, which may contribute to identify new therapeutic targets.

In conclusion, this study reveals the mechanism by which EGCG inhibits hPMCA4 isoform and shows that EGCG can inhibit PMCA activity in living cells. Therefore, the effects of EGCG on Ca^{2+} homeostasis may involve the inhibition of PMCA among other mechanisms.

Declarations

Author contribution statement

Mariela Soledad Ferreira-Gomes: Conceived and designed the experiments; Performed the experiments; Analyzed and interpreted the data; Contributed reagents, materials, analysis tools or data; Wrote the paper.

Débora E. Rinaldi, Mallku Q. Ontiveros: Conceived and designed the experiments; Performed the experiments; Analyzed and interpreted the data.

Nicolas A. Saffioti: Performed the experiments; Analyzed and interpreted the data.

Maximiliano A. Vigil: Performed the experiments.

Irene C. Mangialavori: Analyzed and interpreted the data.

Rolando C. Rossi, Juan P. Rossi: Conceived and designed the experiments; Analyzed and interpreted the data; Contributed reagents, materials, analysis tools or data.

María V. Espelt: Analyzed and interpreted the data; Wrote the paper.

Data availability statement

Data included in article/supplementary material/referenced in article.

Declaration of interests statement

The authors declare no conflict of interest.

Additional information

Supplementary content related to this article has been published online at https://doi.org/10.1016/j.heliyon.2021.e06337.

References

[1] A.N. Panche, A.D. Diwan, S.R. Chandra, Flavonoids: an overview, J. Nutr. Sci. 5 (2016) e47–e47.

[2] S.M. Chacko, P.T. Thambi, R. Kuttan, I. Nishigaki, Beneficial effects of green tea: a literature review, Chin. Med. 5 (2010) 13.

[3] A. Sarkar, V. Tripathi, R. Sahu, Anti-inflammatory and anti-arthritis activity of flavonoids fractions isolated from centipeda minima leaves extracts in rats, Clin. Exp. Pharmacol. 7 (2017) 1–8.

[4] N.P. Bondonno, F. Dalgaard, C. Kyrø, K. Murray, C.P. Bondonno, J.R. Lewis, K.D. Croft, G. Gislason, A. Scalbert, A. Cassidy, A. Tjønneland, K. Overvad, J.M. Hodgson, Flavonoid intake is associated with lower mortality in the Danish Diet Cancer and Health Cohort, Nat. Commun. 10 (2019) 3651.

[5] L. Bartosikova, J. Necas, Epigallocatechin gallate: a review, Vet. Med. 63 (2018) 443–467.

[6] C. Chu, J. Deng, Y. Man, Y. Qu, Green tea extracts epigallocatechin-3-gallate for different treatments, BioMed Res. Int. 2017 (2017) 5615647.

[7] J.-J. Gu, K.-S. Qiao, P. Sun, P. Chen, Q. Li, Study of EGCG induced apoptosis in lung cancer cells by inhibiting PI3K/Akt signaling pathway, Eur. Rev. Med. Pharmacol. Sci. 22 (2018) 4557–4563.

[8] J.D. Lambert, R.J. Elias, The antioxidant and pro-oxidant activities of green tea polyphenols: a role in cancer prevention, Arch. Biochem. Biophys. 501 (2010) 65–72.

[9] C. Mayr, A. Wagner, D. Neureiter, M. Pichler, M. Jakab, R. Illig, F. Berr, T. Kiesslich, The green tea catechin epigallocatechin gallate induces cell cycle arrest and shows potential synergism with cisplatin in biliary tract cancer cells, BMC Compl. Alternative Med. 15 (2015) 194.

[10] K.-J. Min, T.K. Kwon, Anticancer effects and molecular mechanisms of epigallocatechin-3-gallate, Integr. Med. Res. 3 (2014) 16–24.

[11] C. Chu, J. Deng, L. Xiang, Y. Wu, X. Wei, Y. Qu, Y. Man, Evaluation of epigallocatechin-3-gallate (EGCG) cross-linked collagen membranes and concerns on osteoblasts, Mater. Sci. Eng. C Mater. Biol. Appl. 67 (2016) 386–394.

[12] C. Chu, J. Deng, C. Cao, Y. Man, Y. Qu, Evaluation of epigallocatechin-3-gallate modified collagen membrane and concerns on schwann cells, BioMed Res. Int. 2017 (2017) 1–8.

[13] J.-H. Wang, J. Cheng, C.-R. Li, M. Ye, Z. Ma, F. Cai, Modulation of Ca^{2+} signals by epigallocatechin-3-gallate(EGCG) in cultured rat hippocampal neurons, Int. J. Mol. Sci. 12 (2011) 742–754.

[14] H.J. Kim, K.S. Yum, J.-H. Sung, D.-J. Rhie, M.-J. Kim, D.S. Min, S.J. Hahn, M.-S. Kim, Y.-H. Jo, S.H. Yoon, Epigallocatechin-3-gallate increases intracellular [Ca2+] in U87 cells mainly by influx of extracellular Ca2+ and partly by release of intracellular stores, Naunyn-Schmiedeberg's Arch. Pharmacol. 369 (2004) 260–267.

[15] C. Marchetti, P. Gavazzo, B. Burlando, Epigallocatechin-3-gallate mobilizes intracellular Ca2+ in prostate cancer cells through combined Ca2+ entry and Ca2+-induced Ca2+ release, Life Sci. 258 (2020) 118232.

[16] R. Bagur, G. Hajnoczky, Intracellular Ca(2+) sensing: its role in calcium homeostasis and signaling, Mol. Cell. 66 (2017) 780–788.

[17] M. Ontiveros, D. Rinaldi, M. Marder, M. V Espelt, I. Mangialavori, M. Vigil, J.P. Rossi, M. Ferreira-Gomes, Natural flavonoids inhibit the plasma membrane Ca(2+)-ATPase, Biochem. Pharmacol. 166 (2019) 1–11.

[18] N. Stafford, C. Wilson, D. Oceandy, L. Neyses, E.J. Cartwright, The plasma membrane calcium ATPases and their role as major new players in human disease, Physiol. Rev. 97 (2017) 1089–1125.

[19] E.E. Strehler, Plasma membrane calcium ATPases as novel candidates for therapeutic agent development, J. Pharm. Pharmaceut. Sci. 16 (2013) 190–206.

[20] M.S. Ferreira-Gomes, R.M. González-Lebrero, M.C. De La Fuente, E.E. Strehler, R.C. Rossi, J.P. Rossi, Calcium occlusion in plasma membrane Ca^{2+}-ATPase, J. Biol. Chem. 286 (37) (2011) 32018–32025.

[21] H. Ochiai, K. Takeda, S. Soeda, et al., Epigallocatechin-3-gallate is an inhibitor of Na+,K+-ATPase by favoring the E1 conformation, Biochem. Pharmacol. 78 (2009) 1069–1074.

[22] F. Soler, M.C. Asensio, F. Fernández-Belda, Inhibition of the intracellular Ca2+ transporter SERCA (Sarco-endoplasmic Reticulum Ca2+-ATPase) by the natural polyphenol epigallocatechin-3-gallate, J. Bioenerg. Biomembr. 44 (2012) 597–605.

[23] M.S. Ferreira-Gomes, I.C. Mangialavori, M.Q. Ontiveros, D.E. Rinaldi, J. Martiarena, S. V Verstraeten, J.P.F.C. Rossi, Selectivity of plasma membrane calcium ATPase (PMCA)-mediated extrusion of toxic divalent cations in vitro and in cultured cells, Arch. Toxicol. 92 (1) (2018) 273–288.

[24] C. V Filomatori, A.F. Rega, On the mechanism of activation of the plasma membrane Ca^{2+}-ATPase by ATP and acidic phospholipids, J. Biol. Chem. 278 (2003) 22265–22271.

[25] T.P. Stauffer, D. Guerini, E. Carafoli, Tissue distribution of the four gene products of the plasma membrane Ca^{2+} pump. A study using specific antibodies, J. Biol. Chem. 270 (1995) 12184–12190.

[26] D.E. Richards, A.F. Rega, P.J. Garrahan, Two classes of site for ATP in the Ca2+-ATPase from human red cell membranes, Biochim. Biophys. Acta 511 (1978) 194–201.

[27] C. Fiske, Y. Subbarow, The colorimetric determination of phosphorus, J. Biol. Chem. 66 (1925) 375–400.

[28] S.P.J. Brooks, K.B. Storey, Bound and determined: a computer program for making buffers of defined ion concentrations, Anal. Biochem. 201 (1992) 119–126.

[29] M.M. Echarte, V. Levi, A. Villamil, R. Rossi, J. Rossi, Quantitation of plasma membrane calcium pump phosphorylated intermediates by electrophoresis, Anal. Biochem. 289 (2) (2001) 267–273.

[30] J.G. Norby, I. Klodos, N.O. Christiansen, Kinetics of Na-ATPase activity by the Na,K pump. Interactions of the phosphorylated intermediates with Na+, Tris+, and K+. J. Gen. Physiol. 82 (1983) 725–759.

[31] H.J. Schatzmann, S. Luterbacher, J. Stieger, A. Wuthrich, Red blood cell calcium pump and its inhibition by vanadate and lanthanum, J. Cardiovasc. Pharmacol. 8 (Suppl 8) (1986) S33–S37.

[32] H. Akaike, A new look at the statistical model identification, IEEE Trans. Automat. Contr. 19 (1974) 716–723.

[33] B. Webb, A. Sali, Comparative protein structure modeling using MODELLER, Curr. Protoc. Bioinforma. 47 (2014), 5.6.1-32.

[34] D. Gong, X. Chi, K. Ren, G. Huang, G. Zhou, N. Yan, J. Lei, Q. Zhou, Structure of the human plasma membrane Ca(2+)-ATPase 1 in complex with its obligatory subunit neuroplastin, Nat. Commun. 9 (2018) 3623.

[35] G.M. Morris, R. Huey, W. Lindstrom, M.F. Sanner, R.K. Belew, D.S. Goodsell, A.J. Olson, AutoDock4 and AutoDockTools4: automated docking with selective receptor flexibility, J. Comput. Chem. 30 (2009) 2785–2791.

[36] O. Trott, A.J. Olson, AutoDock Vina, Improving the speed and accuracy of docking with a new scoring function, efficient optimization, and multithreading, J. Comput. Chem. 31 (2010) 455–461.

[37] E.F. Pettersen, T.D. Goddard, C.C. Huang, G.S. Couch, D.M. Greenblatt, E.C. Meng, T.E. Ferrin, UCSF Chimera–a visualization system for exploratory research and analysis, J. Comput. Chem. 25 (2004) 1605–1612.

[38] M.C. Chicka, E.E. Strehler, Alternative splicing of the first intracellular loop of plasma membrane Ca^{2+}-ATPase isoform 2 alters its membrane targeting, J. Biol. Chem. 278 (20) (2003) 18464–18470.

[39] O. Thastrup, P.J. Cullen, B.K. Drøbak, M.R. Hanley, A.P. Dawson, Thapsigargin, a tumor promoter, discharges intracellular Ca^{2+} stores by specific inhibition of the endoplasmic reticulum Ca$^{2(+)}$-ATPase, Proc. Natl. Acad. Sci. U. S. A 87 (7) (1990) 2466–2470.

[40] M.G. Dalghi, M. Ferreira-Gomes, N. Montalbetti, A. Simonin, E.E. Strehler, M.A. Hediger, J.P. Rossi, Cortical cytoskeleton dynamics regulates plasma membrane calcium ATPase isoform-2 (PMCA2) activity, Biochim. Biophys. Acta 1864 (8) (2017) 1413–1424.

[41] A.J. Caride, A.G. Filoteo, A. Enyedi, A.K. Verma, J.T. Penniston, Detection of isoform 4 of the plasma membrane calcium pump in human tissues by using isoform-specific monoclonal antibodies, Biochem. J. 316 (Pt 1) (1996) 353–359.

[42] T. Takahashi, S. Nagatoishi, D. Kuroda, K. Tsumoto, Thermodynamic and computational analyses reveal the functional roles of the galloyl group of tea catechins in molecular recognition, PloS One 13 (2018), e0204856.

[43] Y. Shimamura, M. Utsumi, C. Hirai, S. Nakano, S. Ito, A. Tsuji, T. Ishii, T. Hosoya, T. Kan, N. Ohashi, S. Masuda, Binding of catechins to staphylococcal enterotoxin A, Molecules 23 (2018).

[44] C.J. Herscher, A.F. Rega, Pre-steady-state kinetic study of the mechanism of inhibition of the plasma membrane Ca$^{(2+)}$-ATPase by lanthanum, Biochemistry 35 (47) (1996) 14917–14922.

[45] M. Nyblom, H. Poulsen, P. Gourdon, L. Reinhard, M. Andersson, E. Lindahl, N. Fedosova, P. Nissen, Crystal structure of Na+, K(+)-ATPase in the Na(+)-bound state, Science 342 (2013) 123–127.

[46] C. Toyoshima, Structural aspects of ion pumping by Ca2+-ATPase of sarcoplasmic reticulum, Arch. Biochem. Biophys. 476 (2008) 3–11.

[47] F. Pires, V.P.N. Geraldo, A. Antunes, A. Marletta, O.N.J. Oliveira, M. Raposo, On the role of epigallocatechin-3-gallate in protecting phospholipid molecules against UV irradiation, Colloids Surf. B Biointerfaces 173 (2019) 312–319.

[48] F. Pires, G. Magalhães-Mota, V.P.N. Geraldo, P.A. Ribeiro, O.N.J. Oliveira, M. Raposo, The impact of blue light in monolayers representing tumorigenic and nontumorigenic cell membranes containing epigallocatechin-3-gallate, Colloids Surf. B Biointerfaces 193 (2020) 111129.

[49] B. Sarkadi, I. Szasz, G. Gardos, Characteristics and regulation of active calcium transport in inside-out red cell membrane vesicles, BBA - Biomembr. 598 (1980) 326–338.

[50] G.R. Corradi, H.P. Adamo, Intramolecular fluorescence resonance energy transfer between fused autofluorescent proteins reveals rearrangements of the N- and C-terminal segments of the plasma membrane Ca^{2+} pump involved in the activation, J. Biol. Chem. 282 (2007) 35440–35448.

[51] M.J. Berridge, M.D. Bootman, H.L. Roderick, Calcium signalling: dynamics, homeostasis and remodelling, Nat. Rev. Mol. Cell Biol. 4 (2003) 517–529.

[52] K. Pászty, A.J. Caride, Ž. Bajzer, C.P. Offord, R. Padányi, L. Hegedűs, K. Varga, E.E. Strehler, A. Enyedi, Plasma membrane Ca^{2+}-ATPases can shape the pattern of Ca^{2+} transients induced by store-operated Ca^{2+} entry, Sci. Signal. 8 (364) (2015) ra19 LP-ra19.

[53] R. Ficarella, F. Di Leva, M. Bortolozzi, S. Ortolano, F. Donaudy, M. Petrillo, S. Melchionda, A. Lelli, T. Domi, L. Fedrizzi, D. Lim, G.E. Shull, P. Gasparini, M. Brini, F. Mammano, E. Carafoli, A functional study of plasma-membrane calcium-pump isoform 2 mutants causing digenic deafness, Proc. Natl. Acad. Sci. U. S. A 104 (2007) 1516–1521.

[54] J. Hong, H. Lu, X. Meng, et al., Stability , Cellular Uptake , Biotransformation , and Efflux of Tea Polyphenol (−)-Epigallocatechin-3-Gallate in HT-29 Human Colon Adenocarcinoma Cells Stability , Cellular Uptake , Biotransformation , and Efflux of Tea Polyphenol, 2002, pp. 7241–7246.

[55] W. Dai, C. Ruan, Y. Zhang, J. Wang, J. Han, Z. Shao, Y. Sun, J. Liang, Bioavailability enhancement of EGCG by structural modification and nano-delivery: a review, J. Funct. Foods. 65 (2020) 103732.

[56] S. Ishii, H. Kitazawa, T. Mori, A. Kirino, S. Nakamura, N. Osaki, A. Shimotoyodome, I. Tamai, Identification of the catechin uptake transporter responsible for intestinal absorption of epigallocatechin gallate in mice, Sci. Rep. 9 (2019) 11014.

[57] S. Magi, P. Castaldo, M.L. MacRi, M. Maiolino, A. Matteucci, G. Bastioli, S. Gratteri, S. Amoroso, V. Lariccia, Intracellular calcium dysregulation: implications for alzheimer's disease, BioMed Res. Int. 2016 (2016).

[58] M. Deo, S.H. Weinberg, P.M. Boyle, Calcium dynamics and cardiac arrhythmia, Clin. Med. Insights Cardiol. 11 (2017) 1–4.

[59] G.R. Monteith, D. McAndrew, H.M. Faddy, S.J. Roberts-Thomson, Calcium and cancer: targeting Ca^{2+} transport, Nat. Rev. Cancer. 7 (2007) 519–530.

[60] T.A. Stewart, K.T.D.S. Yapa, G.R. Monteith, Altered calcium signaling in cancer cells, Biochim. Biophys. Acta Biomembr. 1848 (2015) 2502–2511.

[61] C. Cui, R. Merritt, L. Fu, et al., Targeting calcium signaling in cancer therapy, Acta Pharm. Sin. B. 7 (2017) 3–17.

[62] T. Zhong, X. Pan, J. Wang, B. Yang, L. Ding, The regulatory roles of calcium channels in tumors, Biochem. Pharmacol. 169 (2019) 113603.

[63] W.J. Lee, S.J. Roberts-Thomson, G.R. Monteith, Plasma membrane calcium-ATPase 2 and 4 in human breast cancer cell lines, Biochem. Biophys. Res. Commun. 337 (2005) 779–783.

[64] C.S. Aung, W. Ye, G. Plowman, A.A. Peters, G.R. Monteith, S.J. Roberts-Thomson, Plasma membrane calcium ATPase 4 and the remodeling of calcium homeostasis in human colon cancer cells, Carcinogenesis 30 (2009) 1962–1969.

[65] S.J. Roberts-Thomson, Plasma membrane calcium pumps and their emerging roles in cancer, World J. Biol. Chem. 1 (2010) 248.

[66] P. Ribiczey, A. Tordai, H. Andrikovics, A.G. Filoteo, J.T. Penniston, J. Enouf, A. Enyedi, B. Papp, T. Kovacs, Isoform-specific up-regulation of plasma membrane Ca2+ATPase expression during colon and gastric cancer cell differentiation, Cell Calcium 42 (2007) 590–605.

[67] M.C. Curry, N.A. Luk, P.A. Kenny, S.J. Roberts-Thomson, G.R. Monteith, Distinct regulation of cytoplasmic calcium signals and cell death pathways by different plasma membrane calcium ATPase isoforms in MDA-MB-231 breast cancer cells, J. Biol. Chem. 287 (2012) 28598–28608.

[68] D. Grinman, D. AthonvarAngkul, J. Wysolmerski, J. Jeong, Calcium metabolism and breast cancer: echoes of lactation? Curr. Opin. Endocr. Metab. Res. 15 (2020) 63–70.

[69] J. VanHouten, C. Sullivan, C. Bazinet, T. Ryoo, R. Camp, D.L. Rimm, G. Chung, J. Wysolmerski, PMCA2 regulates apoptosis during mammary gland involution and predicts outcome in breast cancer, Proc. Natl. Acad. Sci. U. S. A 107 (2010) 11405–11410.

[70] D. Dang, R. Rao, Calcium-ATPases: gene disorders and dysregulation in cancer, Biochim. Biophys. Acta 1863 (2016) 1344–1350.